J. Fluid Mech. (1991), *vol.* 233, *pp.* 613–631
Printed in Great Britain

Unsteady drag on a sphere at finite Reynolds number with small fluctuations in the free-stream velocity

By RENWEI MEI†, CHRISTOPHER J. LAWRENCE AND RONALD J. ADRIAN

Department of Theoretical & Applied Mechanics, University of Illinois at Urbana-Champaign, 104 South Wright Street, Urbana, IL 61801, USA

(Received 20 March 1990 and in revised form 13 June 1991)

Unsteady flow over a stationary sphere with small fluctuations in the free-stream velocity is considered at finite Reynolds number using a finite-difference method. The dependence of the unsteady drag on the frequency of the fluctuations is examined at various Reynolds numbers. It is found that the classical Stokes solution of the unsteady Stokes equation does not correctly describe the behaviour of the unsteady drag at low frequency. Numerical results indicate that the force increases linearly with frequency when the frequency is very small instead of increasing linearly with the square root of the frequency as the classical Stokes solution predicts. This implies that the force has a much shorter memory in the time domain. The incorrect behaviour of the Basset force at large times may explain the unphysical results found by Reeks & Mckee (1984) wherein for a particle introduced to a turbulent flow the initial velocity difference between the particle and fluid has a finite contribution to the long-time particle diffusivity. The added mass component of the force at finite Reynolds number is found to be the same as predicted by creeping flow and potential theories. Effects of Reynolds number on the unsteady drag due to the fluctuating free-stream velocity are presented. The implications for particle motion in turbulence are discussed.

1. Introduction

A small spherical particle suspended in a turbulent flow experiences both steady and unsteady forces. The equation describing the particle motion in the Stokes flow regime under these forces has recently been derived based on the first principles of mechanics by Maxey & Riley (1983). With the Faxén forces neglected, Maxey & Riley's equation is

$$\tfrac{4}{3}\pi a^3\rho_{\mathrm{p}}\frac{\mathrm{d}\boldsymbol{v}}{\mathrm{d}t'} = \tfrac{4}{3}\pi a^3(\rho_{\mathrm{p}}-\rho_{\mathrm{f}})\boldsymbol{g} + 6\pi\mu a(\boldsymbol{u}-\boldsymbol{v}) + 6\pi\mu a^2\int_{-\infty}^{t'}\frac{\mathrm{d}(\boldsymbol{u}-\boldsymbol{v})}{\mathrm{d}\tau}\frac{\mathrm{d}\tau}{[\pi\nu(t'-\tau)]^{\frac{1}{2}}} + \tfrac{2}{3}\pi a^3\rho_{\mathrm{f}}\frac{\mathrm{d}(\boldsymbol{u}-\boldsymbol{v})}{\mathrm{d}t'} + \tfrac{4}{3}\pi a^3\rho_{\mathrm{f}}\frac{\mathrm{D}\boldsymbol{u}}{\mathrm{D}t'}, \quad (1)$$

where ρ_{p}, ρ_{f}, $\boldsymbol{v}$ and $\boldsymbol{u}$ are the densities and the velocities of the particle and the fluid, a is the particle radius, μ and ν are the dynamic and kinematic viscosities of the fluid,

† Present address: Department of Aerospace Engineering, Mechanics and Engineering Science, University of Florida, Gainesville, FL 32611, USA.

$\boldsymbol{g}$ is the gravitational acceleration, and t' is the dimensional time. The first term on the right-hand side is the body force due to gravity and buoyancy; the second is the Stokes drag; the third is the Basset force first derived by Basset (1888) in the time domain, representing the memory effect on the particle motion; the fourth is the force due to the added mass; and the last term results from the acceleration of the local fluid element. Here, $\mathrm{d}/\mathrm{d}t$ refers to the time derivative on the particle trajectory and $\mathrm{D}/\mathrm{D}t = \partial/\partial t + \boldsymbol{u}\cdot\boldsymbol{\nabla}$ refers to the acceleration evaluated on the fluid trajectory. The last term in (1) is the same as the resultant force due to the stresses which would be exerted on the surface of a fluid element if it occupied the particle volume. A similar equation was proposed by Tchen (1947) with a minor difference in the last term. The expressions for the Stokes drag, Basset history force and the force due to the added mass in equation (1) can be obtained from the classical Stokes solution of the unsteady Stokes (1851) equation for the flow due to a sinusoidally oscillating sphere in an otherwise quiescent fluid. The unsteady drag in such a situation can be found in Landau & Lifshitz (1959, p. 96) as

$$F = 6\pi\mu a U_0 \mathrm{e}^{-\mathrm{i}\omega t'}[1 + (1-\mathrm{i})\,(\omega a^2/2\nu)^{\frac{1}{2}} - \mathrm{i}\tfrac{2}{9}\omega a^2/2\nu], \tag{2}$$

where U_0 and ω are the amplitude and frequency of the oscillation. The first term inside the square bracket corresponds to the instantaneous Stokes drag. It is independent of ω. The second term is the Basset force in the frequency domain. It is proportional to the square root of the frequency. The third term is the force due to the added mass, and it is proportional to the frequency. Fourier transformation of (2) leads to the corresponding expression for the unsteady drag in the time domain as it appears in (1).

Maxey & Riley's equation (1), or Tchen's equation, has been widely used as a basic starting point to study the motion of very small particles in general, particularly in turbulent flows, though the results of Auton, Hunt & Prud'homme (1988) for inviscid flow suggest that the fluid acceleration in the added mass term, $\mathrm{d}\boldsymbol{u}/\mathrm{d}t$, should be replaced by $\mathrm{D}\boldsymbol{u}/\mathrm{D}t$ at large Reynolds number Re. In a recent paper by Reeks & Mckee (1984), the influence of the Basset force on particle dispersion in turbulence was investigated. It was found that when the Basset force was kept in the equation governing the particle motion, the velocity difference between the fluid and the particle at the instant when the particle was introduced to the flow has a finite contribution to the long-time particle diffusivity (i.e. the particle dispersion coefficient) which characterizes the tendency of the particle to disperse in the turbulent flow field.

This 'phenomenon' is rather unphysical. While the initial disturbance may influence the individual particle trajectory, it should have negligible effect after a long period of time and, on average, should not affect the ability of the particle to disperse in turbulence. Since the influence of the initial disturbance on the long-time diffusivity is absent when only the Stokes drag and the constant body force are considered, it is apparent that the Basset force term, as it appears in (1), causes the initial disturbance to contribute to the long-time diffusivity. As shown by Reeks & Mckee (1984), the integration kernel, $(t-\tau)^{-\frac{1}{2}}$, causes the contribution of the initial velocity difference to decay like $t^{-\frac{1}{2}}$ as $t\to\infty$, while the displacement of the particle grows as $t^{\frac{1}{2}}$ when $t\to\infty$. An apparent diffusivity results since the diffusivity is equal to the ensemble average of the product of the velocity and the displacement.

It has been suggested that part of the contribution to the long-time diffusivity found in the analysis of Reeks & Mckee (1984) could be associated with an additional term that is needed in Maxey & Riley's equation to account for a non-zero initial

velocity difference (M. R. Maxey 1990, private communication). However, Reeks & Mckee's (1984) arguments compellingly suggest that the slow decay of the Basset term kernel would continue to create a finite contribution that arises from velocity differences that exist at times beyond the initial starting transient.

The foregoing considerations naturally bring the validity of the expression for the Basset force in (1) into question. From the physical point of view, it seems that the memory of the Basset force term is too long, and the initial transient does not decay fast enough at large time. In fact, it is found by Ockendon (1968) that a valid, low-Reynolds-number asymptotic expansion in the large-time limit gives an unsteady drag much different from that predicted by the unsteady Stokes equation. Sano (1981) considered the unsteady flow field induced by a sudden translation of a sphere, which maintains a constant velocity afterwards, at low Reynolds number using a matched asymptotic expansion. He found that the drag on the sphere decays as $t^{-\frac{1}{2}}$ initially, as the Basset solution predicts, and as t^{-2} at large time. This particular case clearly suggests that the Basset force in (1) is not uniformly valid for all times.

Since the unsteady drag in the time domain can be obtained through Fourier transformation of the unsteady drag in the frequency domain in the Stokes flow regime, and the large-time behaviour is dictated by the low-frequency behaviour, the question must focus on the low-frequency behaviour of the unsteady drag, especially the second term in (2), which is the Basset force coefficient in the frequency domain. Specifically,

(i) does the frequency-dependent part of the drag coefficient go to zero as $\omega^{\frac{1}{2}}$ when $\omega \to 0$ as the Stokes solution predicts?

(ii) If not, what causes the behaviour to be different from the Stokes solution and what is the correct behaviour of the Basset force at very small frequency?

(iii) What is the correct behaviour of the memory term in the time domain? In particular, if, as we expect, the true memory kernel has to decay faster than $t^{-\frac{1}{2}}$ in order to avoid having a finite contribution to the diffusivity from the initial disturbance, how fast does the disturbance decay at large time?

(iv) Since cases for Re larger than one are often encountered in engineering applications, how does the unsteady drag behave as Re increases?

In this paper, questions (i), (ii) and (iv) will be answered using a finite-difference solution of the unsteady Navier–Stokes equation for uniform flow over a stationary sphere at finite Reynolds number with small fluctuations in the magnitude of the free-stream velocity. The dimensionless unsteady Navier–Stokes equation is examined. A brief discussion of the relative importance of the three terms, i.e. the unsteady, convection and diffusion terms, indicates that complete neglect of the convection term in the entire flow field at low Reynolds number leads to incorrect behaviour of the unsteady drag at very small frequency. The solution to the unsteady flow field is then obtained by decomposing the solution into a steady part and a fluctuating part which is much smaller in amplitude than the steady one. The equation which governs the fluctuating flow field can therefore be linearized and the resulting fluctuating flow field remains a single harmonic. Both the steady and unsteady parts are solved using a finite-difference technique developed by Mei & Plotkin (1986). The dependence of the unsteady drag on the frequency of the fluctuation is examined for frequencies ranging from zero to values where the asymptotic behaviour can be observed.

From the numerical results, it is found that the unsteady drag due to the fluctuation can be further decomposed into three parts: a quasi-steady component which is a nonlinear function of Re and is independent of frequency; a force due to

the added mass and the acceleration of the stream velocity which is linearly proportional to the frequency and is independent of Re; and the modified Basset force which increases with frequency and decreases as Re increases. The modified Basset force increases linearly with frequency ω when the frequency is very low and increases asymptotically as the square root of frequency, $\omega^{\frac{1}{2}}$, when the frequency is large. This means that the classical Basset force obtained by solving the unsteady Stokes equation is valid only at asymptotically high frequency when one considers small but non-zero Reynolds number. Therefore the integral expression of the Basset history force in the time domain, as it appears in (1), is valid only for the relatively short time period of $(t'-\tau)$. In terms of the long-time behaviour, the modified Basset force in the integral form should have a kernel which decays faster than $(t'-\tau)^{-\frac{1}{2}}$.

It is also found that the force due to the added mass in the present finite-Reynolds-number ($0.1 \leqslant Re \leqslant 40$) case is the same as predicted by creeping flow and potential flow theories and remains a useful concept in this range of Re. As the Reynolds number increases, the computed Basset force decreases for any fixed Stokes number, $\epsilon = (\omega a^2/2\nu)^{\frac{1}{2}}$, with the Stokes solution being the upper bound. The results of the present study can also be used to assess the influence of turbulence on the drag of a sphere which is either fixed or settling in a turbulent flow.

In a subsequent paper, the remaining question (iii) raised above will be addressed. A matched asymptotic solution of the same problem but at low Reynolds number and very small Strouhal number, with correspondingly low frequency, is obtained. The combination of this solution, the present results, and the Stokes solution for the unsteady Stokes equation at large Strouhal number, or high frequency, will be used to approximate the unsteady drag in the time domain.

2. Formulation

2.1. *Inadequacy of the Stokes equation for low-frequency unsteady flow*

In what follows, we consider an unsteady flow past a stationary sphere with the free-stream velocity being in the form of $U(1+\alpha_1 e^{-i\omega t'})$. In terms of the dimensional stream function–vorticity, (ψ', ζ'), formulation, the unsteady Navier–Stokes equation for axisymmetric flow in spherical coordinates (r', θ, ϕ) is

$$\frac{\partial}{\partial t'}(\zeta' r' \sin\theta) + \sin\theta\left[\frac{\partial \psi'}{\partial r'}\frac{\partial}{\partial \theta}\left(\frac{\zeta'}{r'\sin\theta}\right) - \frac{\partial \psi'}{\partial \theta}\frac{\partial}{\partial r'}\left(\frac{\zeta'}{r'\sin\theta}\right)\right] = \nu \mathscr{D}'^2(\zeta' r' \sin\theta), \quad (3a)$$

$$\mathscr{D}'^2 \psi' = \zeta' r' \sin\theta \quad (3b)$$

with

$$\mathscr{D}'^2 = \frac{\partial^2}{\partial r'^2} + \frac{\sin\theta}{r'^2}\frac{\partial}{\partial\theta}\left(\frac{1}{\sin\theta}\frac{\partial}{\partial\theta}\right). \quad (4)$$

The boundary conditions for ψ' and ζ' are

$$\psi' = \frac{\partial \psi'}{\partial r'} = 0 \qquad \text{on} \quad r' = a, \quad (5a)$$

$$\psi' = \zeta' = 0 \qquad \text{on} \quad \theta = 0 \text{ and } \pi, \quad (5b)$$

$$\psi' \to \tfrac{1}{2}U(1+\alpha_1 e^{-i\omega t'}) r'^2 \sin^2\theta \quad \text{as} \quad r' \to \infty. \quad (5c)$$

We introduce the following dimensionless quantities:

$$r = r'/a, \quad t = t'\omega, \quad u = u'/U, \quad \psi = \psi'/(Ua^2), \quad \zeta = \zeta' a/U, \quad \mathscr{D}^2 = a^2 \mathscr{D}'^2 \quad (6)$$

and define

$$y = r\sin\theta, \quad g = \zeta y. \quad (7a, b)$$

Then (3) becomes

$$St\frac{\partial g}{\partial t}+\sin\theta\left[\frac{\partial\psi}{\partial r}\frac{\partial}{\partial\theta}\left(\frac{g}{y^2}\right)-\frac{\partial\psi}{\partial\theta}\frac{\partial}{\partial r}\left(\frac{g}{y^2}\right)\right]=\frac{2}{Re}\mathscr{D}^2 g \tag{8a}$$

$$\mathscr{D}^2\psi = g, \tag{8b}$$

and the boundary conditions are

$$\psi=\frac{\partial\psi}{\partial r}=0 \qquad \text{on} \quad r=1 \tag{9a}$$

$$\psi=g=0 \qquad \text{on} \quad \theta=0 \text{ and } \pi \tag{9b}$$

$$\psi\to\tfrac{1}{2}(1+\alpha_1 e^{-it})r^2\sin^2\theta \quad \text{as} \quad r\to\infty. \tag{9c}$$

In (8*a*),

$$Re=U2a/\nu, \quad St=\omega a/U \tag{10}$$

are the Reynolds number based on the steady stream velocity and the diameter of the sphere, and the Strouhal number based on the frequency of the oscillation and the radius of the sphere.

At this point, (8*a*) is often approximated by neglecting the nonlinear inertial term in comparison with the viscous term for $Re \ll 1$. The resulting linear unsteady Stokes equation can then be solved for arbitrary unsteady motion of the sphere. The Stokes (1851) solution for flow due to a single harmonic oscillation of a sphere is only a special case for a simple geometry executing a simple motion. Unsteady motions of complex geometries, such as prolate and oblate spheroids, circular disk or other axisymmetric bodies, have been studied using the unsteady Stokes equation, as in Kanwal (1955), Lai & Mockros (1972), Lai (1973), and Lawrence & Weinbaum (1986, 1988). The solutions were generally sought in the frequency domain. The unsteady drag or torque due to single harmonic translation or rotation is then Fourier transformed to obtain the unsteady drag in the time domain for arbitrary motion. However, in doing so, it is implicitly assumed that the unsteady term, which is multiplied by the Strouhal number in (8*a*), is much larger than the nonlinear inertial term. For a fixed Reynolds number, no matter how small, there is always a lower limit on *St* below which the nonlinear term cannot be neglected in the whole flow field in comparison with the unsteady term. Below that limit, both have to be neglected for consistency in comparison with the viscous term in the region of the flow field close to the sphere. This will be discussed in more detail in a subsequent paper.

The inadequacy of the Stokes equation for the unsteady problem is now clear. When the drag in the time domain is sought through Fourier transformation, the drag in the frequency domain is needed for all values of ω. However, the behaviour of the drag at very low frequency may be given incorrectly by the solution of the unsteady Stokes equation. This leads directly to the incorrect behaviour of the Basset force term at large times, and causes the initial disturbance to give a finite contribution to the particle diffusivity.

2.2. *Decomposition of the solution*

As stated previously, a small-amplitude fluctuation in the free-stream velocity is considered, $\alpha_1 \ll 1$. A regular perturbation scheme for the flow field is therefore possible for (8) and (9), as has been used by Lighthill (1954) and Ackerberg & Phillips (1972) to study unsteady boundary layers with small fluctuations in the magnitude of the free-stream velocity. Let

$$\psi(r,\theta,t)=\psi_s(r,\theta)+\alpha_1 e^{-it}\psi_1(r,\theta)+O(\alpha_1^2), \tag{11a}$$

$$g(r,\theta,t)=g_s(r,\theta)+\alpha_1 e^{-it}g_1(r,\theta)+O(\alpha_1^2). \tag{11b}$$

From equation (8), the equations for the steady flow solution are

$$\sin\theta\left[\frac{\partial\psi_s}{\partial r}\frac{\partial}{\partial\theta}\left(\frac{g_s}{y^2}\right)-\frac{\partial\psi_s}{\partial\theta}\frac{\partial}{\partial r}\left(\frac{g_s}{y^2}\right)\right]=\frac{2}{Re}\mathscr{D}^2 g_s, \tag{12a}$$

$$\mathscr{D}^2\psi_s = g_s, \tag{12b}$$

and the equations governing the first-order perturbation are

$$-\mathrm{i}Stg_1+\sin\theta\left[\frac{\partial\psi_s}{\partial r}\frac{\partial}{\partial\theta}\left(\frac{g_1}{y^2}\right)-\frac{\partial\psi_s}{\partial\theta}\frac{\partial}{\partial r}\left(\frac{g_1}{y^2}\right)+\frac{\partial\psi_1}{\partial r}\frac{\partial}{\partial\theta}\left(\frac{g_s}{y^2}\right)-\frac{\partial\psi_1}{\partial\theta}\frac{\partial}{\partial r}\left(\frac{g_s}{y^2}\right)\right]=\frac{2}{Re}\mathscr{D}^2 g_1, \tag{13a}$$

$$\mathscr{D}^2\psi_1 = g_1. \tag{13b}$$

The boundary conditions become

$$\psi_s=\frac{\partial\psi_s}{\partial r}=0 \quad \text{on} \quad r=1, \tag{14a}$$

$$\psi_s = g_s = 0 \quad \text{on} \quad \theta = 0 \text{ and } \pi, \tag{14b}$$

$$\psi_s \to \tfrac{1}{2}r^2\sin^2\theta \quad \text{as} \quad r\to\infty. \tag{14c}$$

and

$$\psi_1=\frac{\partial\psi_1}{\partial r}=\frac{\partial\psi_1}{\partial\theta}=0 \quad \text{on} \quad r=1, \tag{15a}$$

$$\psi_1 = g_1 = 0 \quad \text{on} \quad \theta = 0 \text{ and } \pi, \tag{15b}$$

$$\psi_1 \to \tfrac{1}{2}r^2\sin^2\theta \quad \text{as} \quad r\to\infty. \tag{15c}$$

It should be noted that (12) and (13) are possible only because $\alpha_1 \ll 1$ is assumed, and $O(\alpha_1^2)$ terms in the steady solution are negligible.

2.3. *Coordinate stretching*

The numerical solution is performed in a semicircular (r,θ)-domain of $1 \leqslant r \leqslant 150$ and $0 \leqslant \theta \leqslant \pi$ using 65 grid points in the θ-direction and either 65 or 129 grid points in the r-direction. To make best use of the grid points in the radial direction, a transformation is applied to place more grid points near the surface,

$$r = 1+(r_E-1)\{1-c\tan^{-1}[(1-x_2)\tan(1/c)]\}. \tag{16}$$

Here, x_2 is the normal coordinate in the computation domain with $0 \leqslant x_2 \leqslant 1$. The value $r_E = \exp(5) = 148.413$ is chosen for $Re = 0.1$, 0.2, 1.0, and 5.0 following Dennis & Walker (1970), and Oliver & Chung (1985). For $Re = 10$, and 25, $r_E = \exp(4.5) = 90.013$ is used. For $Re = 50$, 60, 100 and 130 $r_E = \exp(3) = 20.085$ is used. These values of r_E are found to be satisfactory for the Reynolds numbers investigated in this study, i.e. for Re between 0.1 and 130 for steady flows, and between 0.1 and 40 for unsteady flows. The parameter c is an $O(1)$ constant. Smaller values of c result in a denser grid near the sphere and larger values of c result in a more uniform grid distribution in the x_2-direction. The value $c = 0.655$ is used for $Re = 0.1$ and 0.2, and $c = 0.645$ is used for $Re = 1$, 5, 10, 25, 40, 60, 100 and 130.

Computations are carried out in a transformed plane (x_1, x_2) where x_2 is as defined above and x_1 is the unstretched θ-coordinate, $x_1 = \theta$. The equations (12) and (13) for g_s, ψ_s, g_1 and ψ_1 in the (x_1, x_2) coordinate system become

$$h_2\sin x_1\left[\frac{\partial}{\partial x_1}\left(\frac{u_s g_s}{y^2}\right)+\frac{\partial}{\partial x_2}\left(\frac{v_s g_s}{y^2}\right)\right]=\frac{2}{Re}\mathscr{L}^2(g_s), \tag{17a}$$

$$\mathscr{L}^2(\psi_s) = g_s, \tag{17b}$$

and
$$-\mathrm{i}Stg_1+h_2\sin x_1\left[\frac{\partial}{\partial x_1}\left(\frac{u_s g_1+u_1 g_s}{y^2}\right)+\frac{\partial}{\partial x_2}\left(\frac{v_s g_1+v_1 g_s}{y^2}\right)\right]=\frac{2}{Re}\mathscr{L}^2(g_1), \tag{18a}$$

$$\mathscr{L}^2(\psi_1)=g_1, \tag{18b}$$

where
$$\mathscr{L}^2(f)\equiv\left[\frac{\sin x_1}{r^2}\frac{\partial}{\partial x_1}\left(\frac{1}{\sin x_1}\frac{\partial f}{\partial x_1}\right)+h_2\frac{\partial}{\partial x_2}\left(h_2\frac{\partial f}{\partial x_2}\right)\right], \tag{19a}$$

$$u=\frac{\partial\psi}{\partial x_2},\quad v=-\frac{\partial\psi}{\partial x_1} \tag{19b}$$

and
$$h_2=\frac{\partial x_2}{\partial r}. \tag{19c}$$

The boundary conditions (14) and (15) are unchanged, apart from being expressed in the (x_1, x_2) coordinate system.

In (18) g_1 and ψ_1 are complex functions. It is desirable to convert (18) into the equations for the real and imaginary parts,

$$g_1=g_{\mathrm{R}}+\mathrm{i}g_{\mathrm{I}} \tag{20a}$$

$$\psi_1=\psi_{\mathrm{R}}+\mathrm{i}\psi_{\mathrm{I}}. \tag{20b}$$

Equations (18) become

$$Stg_{\mathrm{I}}+h_2\sin x_1\left[\frac{\partial}{\partial x_1}\left(\frac{u_s g_{\mathrm{R}}+u_{\mathrm{R}} g_s}{y^2}\right)+\frac{\partial}{\partial x_2}\left(\frac{v_s g_{\mathrm{R}}+v_{\mathrm{R}} g_s}{y^2}\right)\right]=\frac{2}{Re}\mathscr{L}^2(g_{\mathrm{R}}), \tag{21a}$$

$$-Stg_{\mathrm{R}}+h_2\sin x_1\left[\frac{\partial}{\partial x_1}\left(\frac{u_s g_{\mathrm{I}}+u_{\mathrm{I}} g_s}{y^2}\right)+\frac{\partial}{\partial x_2}\left(\frac{v_s g_{\mathrm{I}}+v_{\mathrm{I}} g_s}{y^2}\right)\right]=\frac{2}{Re}\mathscr{L}^2(g_{\mathrm{I}}), \tag{21b}$$

$$\mathscr{L}^2(\psi_{\mathrm{R}})=g_{\mathrm{R}},\quad \mathscr{L}^2(\psi_{\mathrm{I}})=g_{\mathrm{I}}. \tag{21c,d}$$

2.4. *Numerical algorithm*

The finite-difference technique is applied using the time-dependent approach developed by Mei & Plotkin (1986) for steady problems. An artificial time derivative $\partial/\partial t$ is introduced into (17*a*) and (21*a*, *b*) to convert the system from purely elliptic in space into parabolic in time and space. The discretized form of (17*a*) is

$$\begin{aligned}
&\frac{g^{n+1}_{s_{i,j}}-g^{n}_{s_{i,j}}}{\Delta t}+h_{2j}\sin x_{1_i}\left[\left(\frac{u^n_{s_{i+1,j}}g^n_{s_{i+1,j}}}{y^2_{i+1,j}}-\frac{u^n_{s_{i,j}}g^n_{s_{i,j}}}{y^2_{i,j}}+\frac{u^n_{s_{i,j}}g^{n+1}_{s_{i,j}}}{y^2_{i,j}}-\frac{u^n_{s_{i-1,j}}g^{n+1}_{s_{i-1,j}}}{y^2_{i-1,j}}\right)\Big/(2\Delta x_1)\right.\\
&\qquad\left.+\left(\frac{v^n_{s_{i,j+1}}g^n_{s_{i,j+1}}}{y^2_{i,j+1}}-\frac{v^n_{s_{i,j}}g^n_{s_{i,j}}}{y^2_{i,j}}+\frac{v^n_{s_{i,j}}g^{n+1}_{s_{i,j}}}{y^2_{i,j}}-\frac{v^n_{s_{i,j-1}}g^n_{s_{i,j-1}}}{y^2_{i,j-1}}\right)\Big/(2\Delta x_2)\right]\\
&\quad=\frac{2}{Re}\left\{\sin x_{1_i}\left[\frac{g^n_{s_{i+1,j}}-g^{n+1}_{s_{i,j}}}{\sin x_{1_{i+\frac{1}{2}}}}-\frac{g^{n+1}_{s_{i,j}}-g^{n+1}_{s_{i-1,j}}}{\sin x_{1_{i-\frac{1}{2}}}}\right]\Big/(r_j^2\Delta x_1^2)\right.\\
&\qquad\left.+[h_{2_j}(h_{2_{j+\frac{1}{2}}}(g^n_{s_{i,j+1}}-g^{n+1}_{s_{i,j}})-h_{2_{j-\frac{1}{2}}}(g^{n+1}_{s_{i,j}}-g^{n+1}_{s_{i,j-1}}))/\Delta x_2^2]\right\}\\
&\quad\equiv\frac{2}{Re}\mathscr{L}^{2^{n+1}}_{i,j}(g_s).
\end{aligned} \tag{22}$$

Once the steady-state solutions for $(g_{s_{i,j}}, \psi_{s_{i,j}})$ are obtained, they are used in (21*a*, *b*)

as known coefficients to compute $(g_{\mathrm{R}_{i,j}}, \psi_{\mathrm{R}_{i,j}})$ and $(g_{\mathrm{I}_{i,j}}, \psi_{\mathrm{I}_{i,j}})$. The discretized equation for g_{R} is

$$\frac{g^{n+1}_{\mathrm{R}_{i,j}} - g^{n}_{\mathrm{R}_{i,j}}}{\Delta t} + Stg^{n+1}_{\mathrm{I}_{i,j}} + h_{2_j}\sin x_{1_i}\left[\left(\frac{u_{\mathrm{s}_{i+1,j}} g^{n}_{\mathrm{R}_{i+1,j}}}{y^2_{i+1,j}} - \frac{u_{\mathrm{s}_{i,j}} g^{n}_{\mathrm{R}_{i,j}}}{y^2_{i,j}} + \frac{u_{\mathrm{s}_{i,j}} g^{n+1}_{\mathrm{R}_{i,j}}}{y^2_{i,j}} - \frac{u_{\mathrm{s}_{i-1,j}} g^{n+1}_{\mathrm{R}_{i-1,j}}}{y^2_{i-1,j}}\right)\Big/(2\Delta x_1)\right.$$

$$+\left(\frac{v_{\mathrm{s}_{i,j+1}} g^{n}_{\mathrm{R}_{i,j+1}}}{y^2_{i,j+1}} - \frac{v_{\mathrm{s}_{i,j}} g^{n}_{\mathrm{R}_{i,j}}}{y^2_{i,j}} + \frac{v_{\mathrm{s}_{i,j}} g^{n+1}_{\mathrm{R}_{i,j}}}{y^2_{i,j}} - \frac{v_{\mathrm{s}_{i,j-1}} g^{n}_{\mathrm{R}_{i,j-1}}}{y^2_{i,j-1}}\right)\Big/(2\Delta x_2)$$

$$\left.+\left(\frac{u^{n}_{\mathrm{R}_{i+1,j}} g_{\mathrm{s}_{i+1,j}}}{y^2_{i+1,j}} - \frac{u^{n}_{\mathrm{R}_{i-1,j}} g_{\mathrm{s}_{i-1,j}}}{y^2_{i-1,j}}\right)\Big/(2\Delta x_1) + \left(\frac{v^{n}_{\mathrm{R}_{i,j+1}} g_{\mathrm{s}_{i,j+1}}}{y^2_{i,j+1}} - \frac{v^{n}_{\mathrm{R}_{i,j-1}} g_{\mathrm{s}_{i,j-1}}}{y^2_{i,j-1}}\right)\Big/(2\Delta x_2)\right]$$

$$= \frac{2}{Re}\mathscr{L}^{2^{n+1}}_{i,j}(g_{\mathrm{R}}). \tag{23}$$

The rest of the differential equations are treated similarly.

The iteration for g^{n+1}_{s} starts from $(i,j) = (2,2)$ and sweeps from $x_1 = 0$ to $x_1 = \pi$ and from $x_2 = 0$ to $x_2 = 1$, corresponding to $r = r_{\mathrm{E}}$. Therefore the solution for $g_{\mathrm{s}_{i,j}}$ at $(n+1)$ is explicit. However, since the most recently unadapted values at $(i, j-1)$ and $(i-1, j)$ are used in both the convection and diffusion terms in the difference equation, the scheme is, in this sense, semi-implicit. The equations governing $g_{\mathrm{R}_{i,j}}$ and $g_{\mathrm{I}_{i,j}}$ are coupled. Therefore, they are solved as a coupled 2×2 algebraic system. Because of the semi-implicit nature of the finite-difference scheme and the low Reynolds number, the time-step size is not critical. In Cartesian coordinates, the restriction on the time step for a typical convection–diffusion equation is $-\Delta t(u/\Delta x + v/\Delta y) \leqslant 1$, which implies that the time-step size is restricted only for reversed flows (see Mei & Plotkin 1986). For the present case, values of Δt between 0.05 and 0.3 are used for the computations of the vorticity. The convergence is insensitive to the value of Δt in this range because of the coupling of the vorticity on the wall with the stream functions near the wall. The iteration process is stable.

2.5. *Evaluation of wall vorticity and drag*

The function g on the wall, $g_{wi} = g_{i,j-1}$, needs to be updated at every iteration from the latest stream functions near the wall. A second-order-accurate method (Briley 1971) for g_{wi} and $u_{i,j-2}$ is used for the present moderate-Reynolds-number flows,

$$g_{i,1} = 0.5(h_{2_{j-1}}/\Delta x_2)^2 (8\psi_{i,j-2} - \psi_{i,j-3}), \tag{24a}$$

$$u_{i,j-2} = (4\psi_{i,j-2} + \psi_{i,j-3})/(4\Delta x_2). \tag{24b}$$

The dimensional drag on the sphere consists of the frictional drag F'_f due to shear stress and the pressure drag F'_p due to normal stress

$$F' = F'_p + F'_f. \tag{25}$$

The relations between the dimensionless frictional drag $F_f = F'_f/\mu Ua$, the pressure drag $F_p = F'_p/\mu Ua$ and the dimensionless wall vorticity $\zeta = g/y$ are

$$F_f = -2\pi \int_0^{\pi} \zeta|_{r=1} \sin^2\theta \, \mathrm{d}\theta, \tag{26a}$$

$$F_p = -\pi \int_0^{\pi} \sin 2\theta \left[\int_0^{\theta} \left(\frac{\partial \zeta}{\partial r} + \frac{\zeta}{r}\right)_{r=1} \mathrm{d}\theta'\right] \mathrm{d}\theta. \tag{26b}$$

The integrals in (26) are evaluated numerically with second-order accuracy.

3. Results and discussion

For the present problem it is instructive to decompose the total drag into a steady-state drag F'_s and a fluctuating drag $\alpha_1 e^{-i\omega t'} F'_1$,

$$F'(t') = F'_s + \alpha_1 e^{-i\omega t'} F'_1 + O(\alpha_1^2). \tag{27}$$

Since

$$F'_s = 6\pi\mu U a \tag{28}$$

for steady Stokes flow, it is convenient to normalize (27) as

$$\begin{aligned} D(t) &= F'/(6\pi\mu U a) \\ &= D_s(Re) + \alpha_1 e^{-it} D_1(Re, St) \\ &= D_s(Re) + \alpha_1 e^{-it}(D_{1R} + iD_{1I}). \end{aligned} \tag{29}$$

3.1. *Steady drag at finite Re*

In the Stokes regime, $D_s(Re) \to 1$ as $Re \to 0$. The relation between the D_s and Re computed here is shown in figure 1 (*a*). Comparisons of present results with the numerical results of Dennis & Walker (1971), Le Clair, Hamielec & Pruppacher (1970), and Fornberg (1988) are shown in figure 1 (*b*). An empirical correlation

$$D_s = 1 + 0.15 Re^{0.687} \tag{30}$$

given in Clift, Grace & Weber (1978), is also presented. The present numerical results of steady drag at moderate Reynolds number agree well with the earlier published results.

Typical steady flow fields are shown in figure 2 for $Re = 5$, which is an unseparated flow, and for $Re = 40$, and 100 which are separated flows. Figure 3 shows the vorticity distribution on the sphere at various Reynolds numbers along with the results of Dennis & Walker (1971) at $Re = 10$ and Woo (1971) at $Re = 100$ taken from Clift *et al.* (1978).

3.2. *Unsteady drag in the Stokes flow regime*

For an oscillating sphere with velocity $v_1 = \alpha_1 U e^{-i\omega t'}$ in an otherwise steady stream with velocity U in the Stokes flow regime, the fluctuating part of the drag is the same as the solution given in Landau & Lifshitz (1959, p. 96),

$$\alpha_1 \bar{F}'_{1B} = 6\pi\mu a \left[(1+\epsilon) v + \epsilon \left(1 + \frac{2}{9}\epsilon \right) \frac{1}{\omega} \frac{dv}{dt} \right], \tag{31}$$

where

$$\epsilon = (\omega a^2 / 2\nu)^{\frac{1}{2}} = (\tfrac{1}{4} St\, Re)^{\frac{1}{2}}. \tag{32}$$

The overbar indicates that the results are for the oscillating sphere case, and the subscript B means that the solution corresponds to the Stokes solution of the Stokes equation. Consequently,

$$\bar{D}_{1B} = 1 + (1-i)\epsilon - i\tfrac{2}{9}\epsilon^2 \tag{33}$$

for a sphere executing an axial oscillation. In the above, the first term is from the instantaneous Stokes drag, the second term, $(1-i)\epsilon$, is associated with the Basset force, and the last one is the force due to the added mass.

For fluctuating free-stream velocity $U(1 + \alpha_1 e^{-i\omega t'})$ past a stationary sphere, it can

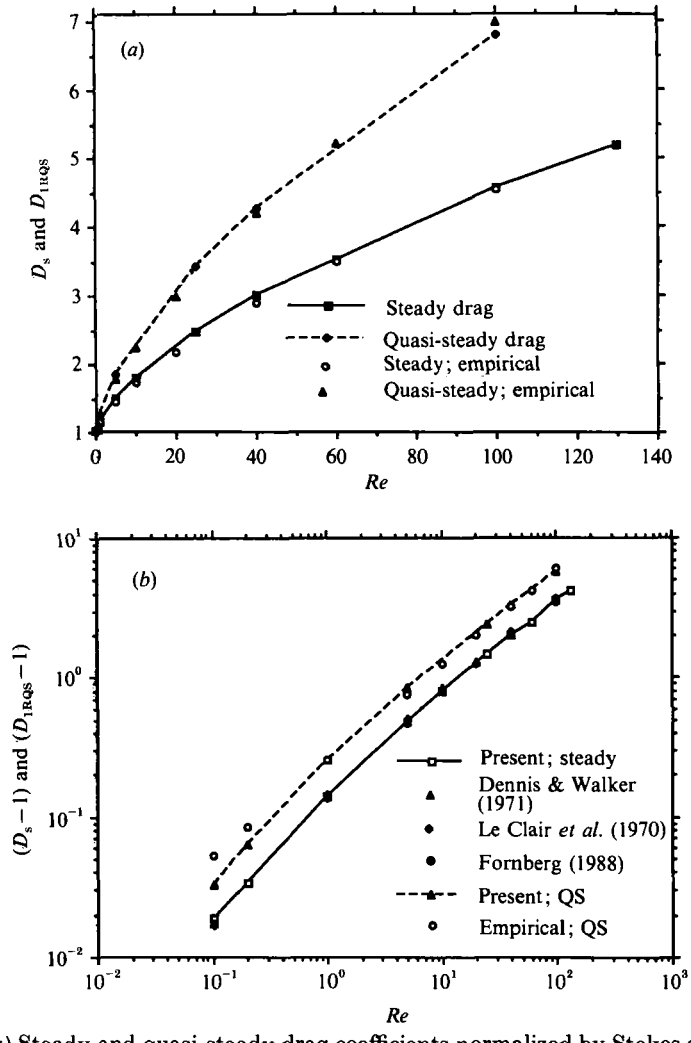

FIGURE 1. (*a*) Steady and quasi-steady drag coefficients normalized by Stokes drag as functions of *Re*. The empirical correlation for the quasi-steady drag is linearized from the steady drag coefficient given in Clift *et al.* (1978). (*b*) Comparisons of the steady and quasi-steady drag coefficients with other numerical and empirical results.

be shown by a coordinate transformation of the complete unsteady Navier–Stokes equation that

$$D_{1B} = 1 + (1 - \mathrm{i})\epsilon - \mathrm{i}\tfrac{2}{9}\epsilon^2 - \mathrm{i}\tfrac{4}{9}\epsilon^2, \tag{34}$$

where the additional term, $-\mathrm{i}\frac{4}{9}\epsilon^2$, results from the fact that the fluid, rather than the body, is oscillating. In the time domain this is $\frac{4}{3}\pi a^3 \rho_f \, \mathrm{d}v/\mathrm{d}t$, and it is independent of *Re*, i.e. it holds for any flow. This term appears as $\frac{4}{3}\pi a^3 \rho_f \, \mathrm{D}u/\mathrm{D}t$ in the equation of motion for particles with very small particle Reynolds number derived by Maxey & Riley (1983) and in the equation of motion for large particles (such as large bubbles in liquid), whose motion relative to the carrier fluid can be approximated as inviscid flow, derived by Auton *et al.* (1988). It accounts for the resultant force due to the total stresses of the undisturbed fluid flow acting on the surface of the sphere. In the present case, the ambient flow surrounding the sphere is assumed uniform. The force associated with $\mathrm{D}u/\mathrm{D}t$ is purely from the fluctuation of the stream velocity.

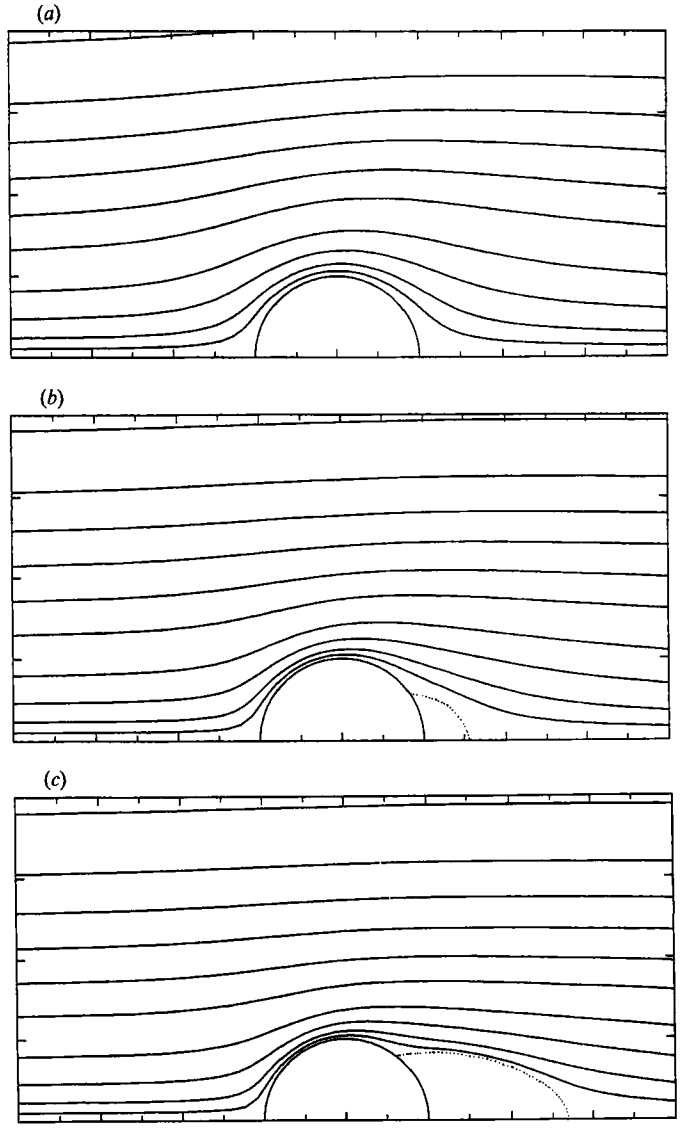

FIGURE 2. Streamlines corresponding to $\psi = 0$, 0.005, 0.025, 0.1, 0.3, 0.8, 1.4, 2.2, 3.2, 4.5 and 7.8 for steady flow past a sphere at (*a*) $Re = 5$; (*b*) $Re = 40$; and (*c*) $Re = 100$.

Consequently, the difference between D_1 and $\bar{D}_1$ or between D_{1B} and $\bar{D}_{1B}$, is $-\mathrm{i}\frac{4}{9}\epsilon^2$. Using the Stokes equation, the Stokes solution for the present case of a fluctuating free-stream velocity leads to

$$\begin{aligned} D_{1B} &= 1+(1-\mathrm{i})\,\epsilon-\mathrm{i}\tfrac{2}{3}\epsilon^2 \\ &= 1+\epsilon-\mathrm{i}(\epsilon+\tfrac{2}{3}\epsilon^2) \\ &= D_{1BR}+\mathrm{i}D_{1BI}. \end{aligned} \tag{35}$$

3.3. *Unsteady drag at finite Re*

The classical Stokes solution (35) is valid for $Re \to 0$ and finite ϵ relative to Re, but arbitrary amplitude of the free-stream oscillation, α_1. In contrast, the present solution is valid for finite Reynolds number (including cases with separated flow), but

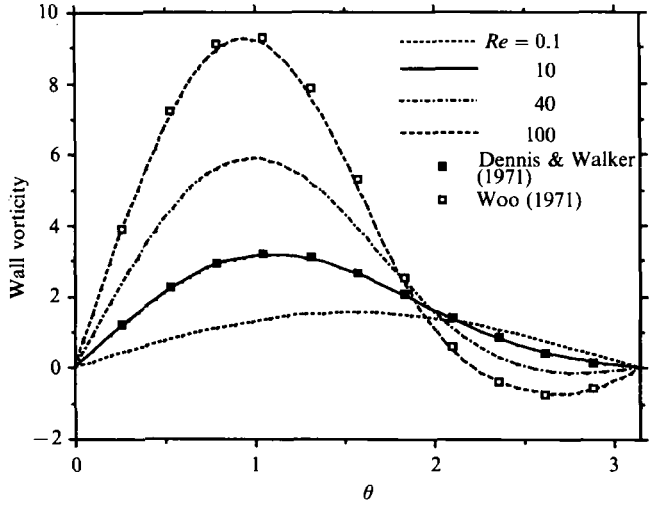

FIGURE 3. Vorticity distribution on the sphere at $Re = 0.1$, 10, 40, and 100. Comparisons are made with Dennis & Walker (1971) at $Re = 10$ and with Woo (1971) at $Re = 100$.

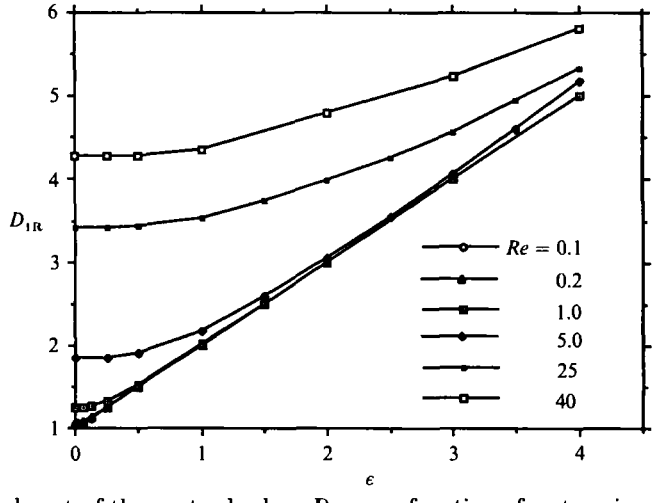

FIGURE 4. Real part of the unsteady drag D_{1R} as a function of ϵ at various Reynolds numbers.

small α_1. We shall discuss the behaviour of the present solution by comparing it directly to the Stokes solution.

The real part of the unsteady drag D_{1R} is shown in figure 4 as a function of ϵ. It can be decomposed into a *quasi-steady* component D_{1RQS} that is defined as the value of D_{1R} at zero frequency, i.e. $\epsilon \to 0$, and a component that depends upon ϵ and hence frequency. We refer to that latter component as the *acceleration-dependent* component D_{1RAC} because its value is determined by the amplitude of dv/dt. For example, the Stokes solution of the unsteady Stokes equation yields an unsteady drag, equation (35), in which the quasi-steady component is $D_{1BRQS} = 1$ and the acceleration-dependent component is $D_{1BRAC} = \epsilon$ corresponding to the real part of the Basset force term. The present solution yields an unsteady drag whose quasi-steady component varies with Reynolds number as shown by the limiting values of the drag in figure 4 as ϵ approaches zero. In general, the quasi-steady drag, D_{1RQS}, is independent of St but depends on Re and it can be obtained by computing the drag

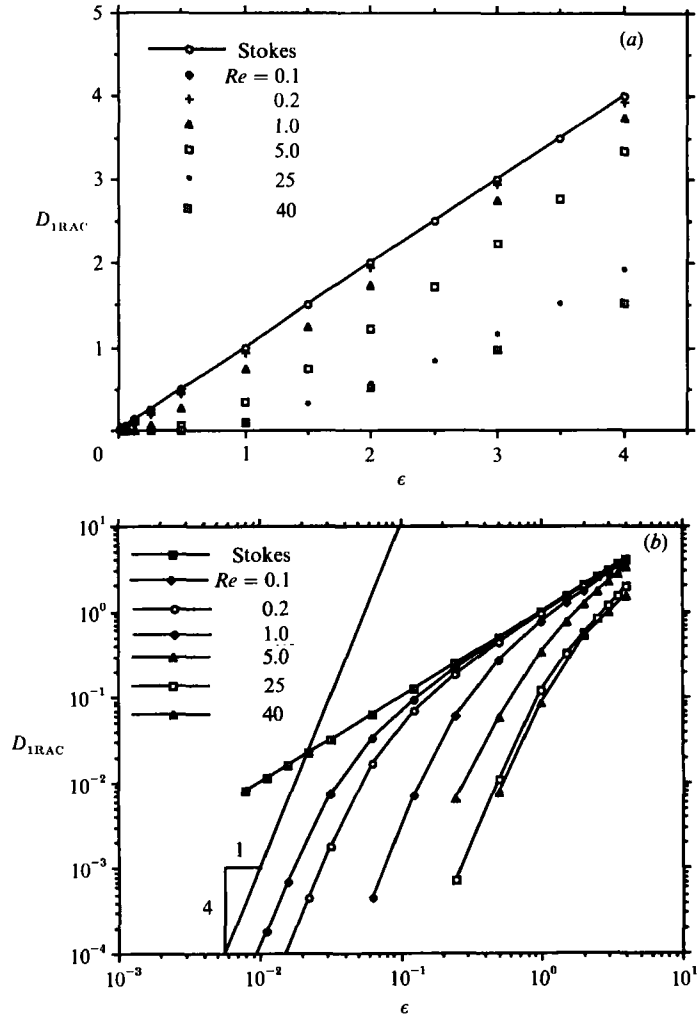

FIGURE 5. Real part of the computed Basset force D_{1RAC} as a function of ϵ at various Reynolds numbers. (*a*) Linear plot; (*b*) log–log plot.

at zero frequency. D_{1RAC} can then be found easily by subtracting D_{1RQS} from D_{1R}. Empirically, D_{1RQS} can be obtained as $D_{1RQS} = 1+0.15(1+0.687)Re^{0.687}$ by linearizing the total drag using the steady-state drag coefficient and the instantaneous velocity

$$6\pi\mu aU(1+\alpha_1 e^{-i\omega t'})\{1+0.15[Re(1+\alpha_1 e^{-i\omega t'})]^{0.687}\}$$

for small α_1. The comparison between the D_{1RQS} computed here and the above empirical result is shown in figure 1 (*a*, *b*). The agreement is close over a large range of Reynolds number, as expected. The deviation at $Re < 1$ is solely the consequence of the poor agreement on a log–log scale between the empirical correlation and the computed steady drag.

In figure 5(*a*), D_{1RAC} is shown as a function of ϵ for different values of Re. It can be seen that for small Reynolds number ($Re \sim 0.1$), D_{1RAC} is indistinguishable from $D_{1BRAC} = \epsilon$, the Stokes solution, at finite values of ϵ. For $Re \geqslant 1.0$, D_{1RAC} is less than $D_{1BRAC} = \epsilon$ for all values of ϵ, and $D_{1RAC} \to D_{1BRAC} = \epsilon$ asymptotically only when

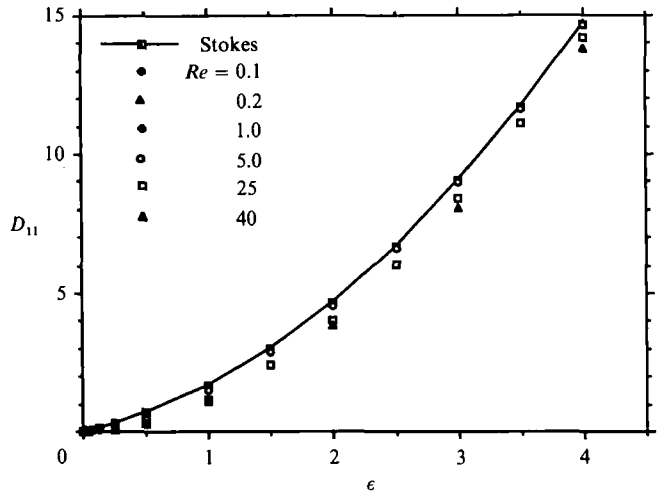

FIGURE 6. Imaginary part of the unsteady drag D_{1I} as a function of ϵ at various Reynolds numbers.

$\epsilon \to \infty$. The difference between D_{1RAC} and D_{1BRAC} as a function of ϵ depends on Re. D_{1RAC} decreases with increasing Reynolds number leading to larger differences with the Basset term. As $\epsilon \to 0$, figure 5(*b*) indicates that D_{1RAC} approaches zero as ϵ^4, much faster than the first-power dependence of the Basset term. Figure 5(*a*, *b*) also shows that the Stokes solution is valid only for relatively large values of ϵ (or ω).

Comparison of the imaginary part of the unsteady drag, D_{1I}, obtained from the unsteady Navier–Stokes equation, with $D_{1BI} = -(\epsilon + \frac{2}{3}\epsilon^2)$ from the Stokes solution is revealing. For large ϵ, $D_{1BI} \to -\frac{2}{3}\epsilon^2$ asymptotically. Figure 6 shows the computed drag D_{1I} and the Stokes solution D_{1BI} as functions of ϵ for different values of Re. For a fixed Re, the difference between D_{1I} and D_{1BI} at large ϵ is small compared with D_{1BI}. Therefore, both D_{1I} and D_{1BI} have the same asymptote, $-\frac{2}{3}\epsilon^2$. This asymptote, as it appears in figure 6, is the same for all Re. Through coordinate transformation, which is independent of Re, the asymptote for $\bar{D}_{1I}$, the imaginary part of the unsteady drag of an oscillating sphere in a steady stream, can be obtained as $-\mathrm{i}\frac{2}{9}\epsilon^2$. This means that *the force due to the added mass for an oscillating sphere at finite Re in the range investigated here is the same as in the creeping flow regime* ($Re \to 0$) *and in potential flow, at least for high-frequency oscillations*, in contrast to some of the findings about added mass force cited in the review by Torobin & Gauvin (1959) which stated that 'The added mass concept is shown to be both completely inadequate and theoretically unsound'.

If $-\frac{2}{3}\epsilon^2$ is subtracted from the Basset drag D_{1IB} the remainder is $-\epsilon$ for all values of ϵ. In figure 7(*a*), $\Delta_I \equiv -(D_{1I} + \frac{2}{3}\epsilon^2)$ is shown as a function of ϵ for various Reynolds numbers. A trend similar to that observed for D_{1RAC} is observed for Δ_I also. For the Stokes solution, $\Delta_I = \epsilon$ is the imaginary part of the Basset force. For small Re (~ 0.1), the difference between Δ_I and ϵ is indistinguishable graphically for a wide range of finite ϵ. For finite Re, the calculation indicates that Δ_I is consistently less than $\Delta_{IB} = \epsilon$ for all values of ϵ and $\Delta_I \to \Delta_{IB}$ asymptotically as $\epsilon \to \infty$. The difference between Δ_I and Δ_{IB} also depends on Re. It is interesting to note that, for finite Re, Δ_I becomes proportional to ϵ^2 instead of ϵ as $\epsilon \to 0$. Figure 7(*b*) shows Δ_I as a function of ϵ at various Reynolds numbers in log–log coordinates. For small values of ϵ, the ϵ^2 dependence of Δ_I is clear. Figure 7(*c*) is a blow-up of figure 7(*a*) as $\epsilon \to 0$. Again, the

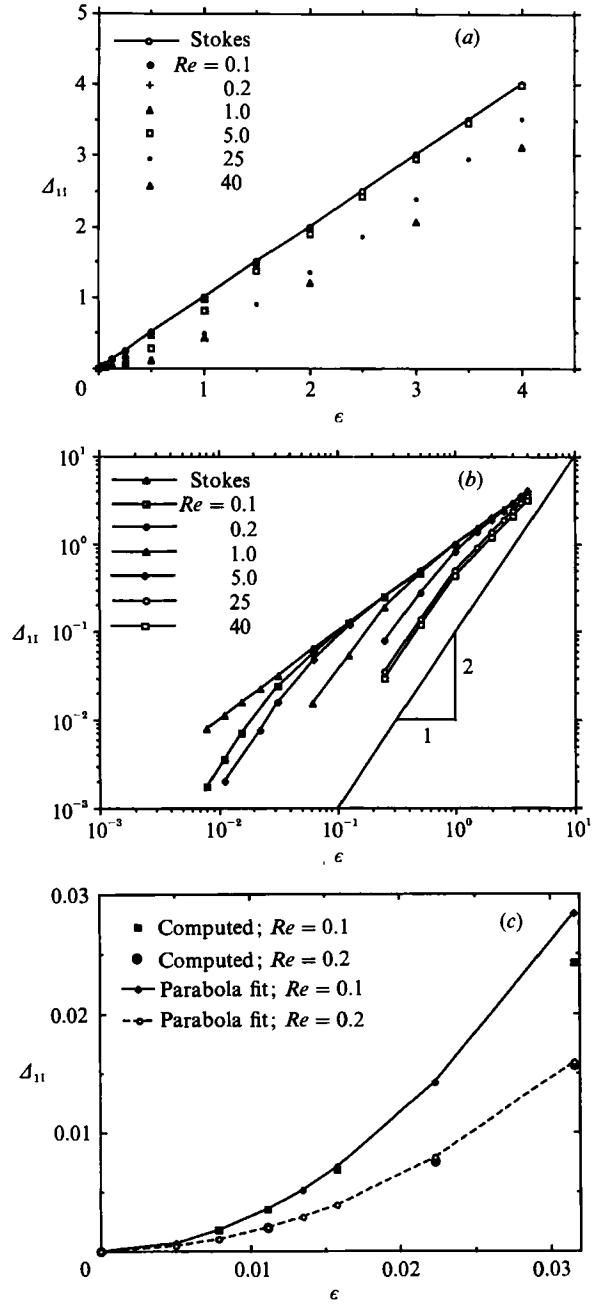

FIGURE 7. Imaginary part of the computed Basset force Δ_{II} as a function of ϵ at various Reynolds numbers. (*a*) Linear plot; (*b*) log–log plot. (*c*) Blow-up of Δ_{II} at small ϵ showing the ϵ^2 dependence of Δ_{II} for $Re = 0.1$ and $Re = 0.2$.

ϵ^2 dependence of Δ_I for small ϵ is clearly demonstrated. The behaviour of D_{1RAC} and Δ_I at small ϵ indicate that the leading-order term of the acceleration-dependent part of D_1 is proportional to the Strouhal number, St, or the frequency ω rather than $\epsilon \sim \omega^{\frac{1}{2}}$ as $St \to 0$ or $\omega \to 0$.

The behaviour of $D_{1\mathrm{RAC}} \sim \epsilon^4 \sim St^2$ and $\Delta_\mathrm{I} \sim \epsilon^2 \sim St$ at small ϵ or St can be explained qualitatively by examining equation (21) for g_R and g_I. For finite Re and very small St (strictly speaking, $St \ll \min(1, Re)$), the solution for g_R and g_1 may be expanded as

$$g_\mathrm{R} = g_{\mathrm{R}1} + St^2 g_{\mathrm{R}2} + \text{h.o.t.}$$

and

$$g_1 = St g_{11} + \text{h.o.t.}$$

$g_{\mathrm{R}1}$ is the quasi-steady solution due to the inhomogeneous boundary conditions at infinity and is $O(1)$. Both g_{11} and $g_{\mathrm{R}2}$ have homogeneous boundary conditions at infinity and the same homogeneous operators (i.e. the spatial derivatives). The leading-order term in g_I, i.e. $St g_{11}$, is solely due to the driving term, $St g_{\mathrm{R}1}$, in (21*b*). The $St^2 g_{\mathrm{R}2}$ term in the expansion of g_R is driven by $St g_\mathrm{I} \sim St^2 g_{11}$ and it can be solved after g_{11} is obtained. Therefore, $D_{1\mathrm{R}} - D_{1\mathrm{RQS}} = D_{1\mathrm{RAC}} = O(St^2)$ and $D_{1\mathrm{I}} = O(St)$ for $St \ll 1$. The leading term of the acceleration-dependent unsteady drag is therefore from the imaginary part $D_{11} = O(St)$.

It should be noted that at very small frequency, the imaginary part of the unsteady drag, D_{11} or Δ_I, approaches an asymptotic limit, $0.75St$, for $St \ll Re \ll 1$. An analysis leading to this asymptotic result using the method of matched asymptotic expansions will be presented in another paper.

The differences in $D_{1\mathrm{RAC}}$ and Δ_1 between the present result and that of the Stokes solution at $\epsilon \ll 1$ may also be explained physically as follows. In the Stokes equation, the diffusion term is balanced by the unsteady term. There are two lengthscales, 1 and $1/\epsilon$, with the radius of the sphere being one. The ratio of the two lengthscales is the Stokes number ϵ. The flow field may be divided into two regions according to ϵ. The vorticity is confined in the region $r-1 \leqslant O(1/\epsilon)$, the Stokes layer. In the region $r-1 > O(1/\epsilon)$, the flow is essentially irrotational. At very low frequency, this Stokes layer is very large. When the nonlinear convection term is included, an additional lengthscale is introduced, i.e. $1/Re$. At low Re, the convection balances the diffusion in transporting the vorticity in the Oseen region, $O(1/Re)$, in the steady state, and the vorticity becomes very small at $r \sim O(1/Re)$. In unsteady flow with very small ϵ, say $\epsilon \ll Re$, the vorticity, which is generated on the wall, is already very small at $r \sim O(1/Re)$. Thus, the Stokes layer, which extends outside the Oseen region, becomes less important to the vorticity transport. The effect of the unsteadiness on the unsteady drag at low but non-zero Reynolds number is, therefore, much smaller than in the case of zero-Reynolds-number unsteady flow. At high frequency, with $\epsilon \gg Re$ if Re is small or $\epsilon \gg Re^{\frac{1}{2}}$ if $Re \gg 1$, the Stokes layer is very small compared with the Oseen region or the boundary layer. Because the vorticity is confined in the Stokes layer where diffusion dominates the vorticity transport, the role of convection diminishes and the unsteady drag can be predicted using the Stokes equation.

When Fourier transformation is applied to obtain the drag in the time domain, the long-time behaviour of the drag based on the full Navier–Stokes equation will be rather different from that predicted by the Stokes solution because of the difference in the small-frequency behaviour (according to the Abelian theorem). Since D_1 is proportional to ω instead of $\omega^{\frac{1}{2}}$, the corresponding Basset force term in the time domain must have a kernel function decaying faster than $(t-\tau)^{-\frac{1}{2}}$, as it appears in (1), for large $(t-\tau)$. However, since $D_{1\mathrm{RAC}}$ and Δ_I are both asymptotically proportional to $\omega^{\frac{1}{2}}$ at high frequency ($\epsilon \to \infty$), the short-time behaviour of the drag should be as predicted by the Basset solution, even for finite Re, i.e. the kernel function behaves as $(t-\tau)^{-\frac{1}{2}}$ for small values of $(t-\tau)$. The appropriate expression for the Basset force in the time domain will be proposed in a subsequent paper, based on a matched

asymptotic solution of the same problem at low Re and very small St, the present results, and the Stokes solution at high frequency.

Since $D_{1\mathrm{RAC}}$ and Δ_{I} are both consistently less than ϵ, it is concluded that the use of the classical Basset force obtained from the Stokes solution of the unsteady Stokes equation would overestimate the actual Basset force for finite Re in both time and frequency domains. This implies that in the studies of particle dispersion in turbulence, where the particle Reynolds number increases as particle inertia gets larger, the effect of the Basset force on the particle motion would decrease when the particle Reynolds number, or the inertia of the particle, increases. Furthermore, as the particle Reynolds number increases, the quasi-steady drag, $D_{1\mathrm{RQS}}$, increases rapidly. This means that the important component of the unsteady drag at large Reynolds number and finite Stokes number, ϵ, is the quasi-steady drag which is determined at zero frequency.

As shown in Mei, Adrian & Hanratty (1991), the classical Basset force derived from the Stokes equation has little effect on the diffusivity of particle motion in general, and it affects only slightly the intensity of particle motion in isotropic turbulence when the particle settling velocity and the Stokes number ϵ are large and the ratio of the particle response time to the turbulence integral timescale is around one. Therefore, its effect on the particle dispersion at larger Reynolds number, or larger inertia, may be neglected, and the quasi-steady drag alone may be sufficient to capture the important features of the unsteadiness of the flow around the particle. Since the quasi-steady drag is derivable by linearizing the steady-state drag, its effect is automatically represented by using the steady-state drag coefficient and the instantaneous relative velocity when the fluctuation in the stream velocity is small.

On the other hand, in some applications, the effect of the Basset force may become critically important and the Basset force must be kept in the equation for particle motion. For example, Leichtberg *et al.* (1976) found a significant effect of the Basset force on the interaction among three coaxially settling spheres at low but non-zero Reynolds numbers. In their study, the Reynolds number is of the order of 0.01 and the $(t-\tau)^{-\frac{1}{2}}$ behaviour of the Basset force may be correct for a period of time which is longer than the whole period of the interaction among the spheres.

4. Conclusions

A finite-difference solution of the Navier–Stokes equation has been obtained for axisymmetric flow over a stationary sphere at finite Reynolds number with small fluctuations in the free-stream velocity. The unsteady drag due to the oscillation in the stream velocity is examined and compared with that found from the classical Stokes solution of the unsteady Stokes equation. At finite Reynolds number the force due to the added mass is the same as in creeping flow and potential flow. The acceleration-dependent force computed at finite Re is linearly proportional to the square root of the frequency only at high frequency (corresponding to the Stokes solution for low Reynolds number motion). At small frequency it is linearly proportional to ω. The classical Stokes solution is not uniformly valid for all ω even for small, non-zero Re. The Basset-force term in the time domain has a kernel which must decay much faster than $(t-\tau)^{-\frac{1}{2}}$ at large time. In the presence of the Basset force, the unphysical result obtained by Reeks & Mckee (1984) wherein the initial velocity difference between the particle and the fluid having a finite contribution to the particle long-time diffusivity may be due to the incorrect behaviour of the classical Basset force at large time. The classical Stokes solution in general seems to

give an 'upper bound' for the unsteady drag coefficient in the frequency domain. As Re increases, the numerically computed Basset force decreases in amplitude ($D_{1\mathrm{RAC}}$ and Δ_1) significantly at small frequencies ($\epsilon \sim 1$) and the Basset force term becomes smaller in comparison with the quasi-steady drag.

The authors wish to thank Professor Thomas J. Hanratty for his encouragement and stimulating discussions. This work was supported by the Multiphase Flow Research Institute through Argonne Contract No. 82862403 and was partially supported by NSF through CBT 88-00980. The computations were performed at the National Center for Supercomputer Applications at the University of Illinois at Urbana-Champaign on a Cray X-MP under a grant from Cray Research, Inc. This paper is based on Chapter 4 of the Ph.D. thesis of the first author while he was at the University of Illinois at Urbana-Champaign.

REFERENCES

ACKERBERG, R. C. & PHILLIPS, J. H. 1972 The unsteady laminar boundary layer on a semi-infinite flat plate due to small fluctuations in the magnitude of the free-stream velocity. *J. Fluid Mech.* **51**, 137–157.

AUTON, T. T., HUNT, J. C. R. & PRUD'HOMME, M. 1988 The force exerted on a body in inviscid unsteady non-uniform rotational flow. *J. Fluid Mech.* **197**, 241–257.

BASSET, A. B. 1888 *A Treatise on Hydrodynamics*, vol. 2. Dover.

BRILEY, M. R. 1971 A numerical study of laminar separation bubbles using the Navier–Stokes equations. *J. Fluid Mech.* **47**, 713–736.

CLIFT, R., GRACE, J. R. & WEBER, M. E. 1978 *Bubbles, Drops and Particles.* Academic.

DENNIS, S. C. R. & WALKER, J. D. A. 1971 Calculation of the steady flow past a sphere at low and moderate Reynolds numbers. *J. Fluid Mech.* **48**, 771–789.

FORNBERG, B. 1988 Steady viscous flow past a sphere at high Reynolds numbers. *J. Fluid Mech.* **190**, 471–489.

KANWAL, R. P. 1955 Rotatory and longitudinal oscillations of axisymmetric bodies in a viscous fluid. *Q. J. Mech. Appl. Maths* **8**, 147–163.

LAI, R. Y. S. 1973 Translatory accelerations of a circular disk in a viscous fluid. *Appl. Sci. Res.* **27**, 441.

LAI, R. Y. S. & MOCKROS, L. F. 1972 The Stokes-flow drag on prolate and oblate spheroids during axial translatory accelerations. *J. Fluid Mech.* **52**, 1–15.

LANDAU, L. E. & LIFSHITZ, E. M. 1959 *Fluid Mechanics.* Pergamon.

LAWRENCE, C. J. & WEINBAUM, S. 1986 The force on an axisymmetric body in linearized, time-dependent motion: a new memory term. *J. Fluid Mech.* **171**, 209–218.

LAWRENCE, C. J. & WEINBAUM, S. 1988 The unsteady force on a body at low Reynolds number; the axisymmetric motion of a spheroid. *J. Fluid Mech.* **189**, 463–489.

LE CLAIR, B. P., HAMIELEC, A. C. & PRUPPACHER, H. R. 1970 A numerical study of the drag on a sphere at low and intermediate Reynolds number. *J. Atmos. Sci.* **27**, 308–315.

LEICHTBERG, S., WEINBAUM, S., PFEFFER, R. & GLUCKMAN, M. J. 1976 A study of unsteady forces at low Reynolds number: a strong interaction theory for the coaxial settling of three or more spheres. *Phil. Trans. R. Soc. Lond.* A **282**, 585–610.

LIGHTHILL, M. J. 1954 The response of laminar skin friction and heat transfer to fluctuations in the stream velocity. *Proc. R. Soc. Lond.* A **224**, 1–23.

MAXEY, M. R. & RILEY, J. J. 1983 Equation of motion for a small rigid sphere in a nonuniform flow. *Phys. Fluids* **26**, 863–889.

MEI, R., ADRIAN, R. J. & HANRATTY, T. J. 1991 Particle dispersion in isotropic turbulence under Stokes drag and Basset force with gravitational settling. *J. Fluid Mech.* **225**, 481–495.

MEI, R. & PLOTKIN, A. 1986 A finite difference scheme for the solution of the steady Navier–Stokes equation. *Comput. Fluids* **14**, 239–251.

OCKENDON, J. R. 1968 The unsteady motion of a small sphere in a viscous liquid. *J. Fluid Mech.* **34**, 229–239.

OLIVER, D. L. R. & CHUNG, J. N. 1985 Steady flows inside and around a fluid sphere at low Reynolds numbers. *J. Fluid Mech.* **154**, 215–230.

REEKS, M. W. & MCKEE, S. 1984 The dispersive effects of Basset history forces on particle motion in a turbulent flow. *Phys. Fluids* **27**, 1573–1582.

SANO, T. 1981 Unsteady flow past a sphere at low Reynolds number. *J. Fluid Mech.* **112**, 433–441.

STOKES, G. G. 1851 On the effect of internal friction of fluids on the motion of pendulum. *Trans. Camb. Phil. Soc.* **9**, 8. (Reprinted in *Mathematical and Physical Papers III.* Cambridge University Press, 1922).

TCHEN, C. M. 1947 Mean value and correlation problems connected with the motion of small particles suspended in a turbulent fluid. Ph.D. thesis, Delft University, Netherlands.

TOROBIN, L. B. & GAUVIN, W. H. 1959 Fundamental aspects of solids–gas flow. Part III. *Can. J. Chem. Engng* **37**, 224–236.

WOO, S. W. 1971 Simultaneous free and forced convection around submerged cylinders and sphere. Ph.D. thesis, McMaster University, Hamilton, Ontario.